LRP 681/00 September 2000

Time-resolved imaging of anodic arc root behavior during fluctuations of a DC plasma spraying torch

J.-L. Dorier, M. Gindrat, Ch. Hollenstein,
A. Salito, M. Loch, G. Barbezat

Submitted for publication in
IEEE Transactions on Plasma Science

ISSN 0458-5895

TIME-RESOLVED IMAGING OF ANODIC ARC ROOT BEHAVIOR DURING FLUCTUATIONS OF A DC PLASMA SPRAYING TORCH

J. -L. Dorier[1], M. Gindrat[1], Ch. Hollenstein[1], A. Salito[2], M. Loch[2] and G. Barbezat[2]

[1] EPFL-Centre de Recherches en Physique des Plasmas, CH-1015 Lausanne, Switzerland,
Phone +41 21 693 34 61, Fax: +41 21 693 51 76, e-mail: jean-luc.dorier@epfl.ch

[2] Sulzer Metco (Switzerland) AG, Rigackerstrasse 16, CH-5610 Wohlen, Switzerland

Index terms: torch, fluctuations, restrike, plasma spraying, arc root, fast imaging

Abstract

The fluctuating behavior of a Sulzer Metco F4 DC plasma gun has been investigated by simultaneous measurement of the time dependencies of the arc voltage and of images from the nozzle interior. An end-on imaging arrangement using a mirror and a mask in the optical path from the arc to the camera allows visualization of the anodic arc attachment by strongly attenuating the bright emission from the arc column. With the torch operating in the restrike mode, sequences of images have been acquired in synchronization with several typical features of the arc voltage fluctuations showing that the attachment nature changes during a restrike cycle. Multiple attachments which co-exist at least during the 1 μs exposure time of the camera have been evidenced and are interpreted as a continuous process of creation/vanishing of successive arc roots with a smooth transfer of the current from one to the other. The anode wear is shown to have a strong effect on the root position over the anode periphery, with a preference for attachment in eroded regions. The effects of operation parameters such as current, gas flow and injector type on the attachment nature and position are also presented.

1. INTRODUCTION

Plasma spraying has been extensively used for producing coatings with special properties in various industrial sectors such as the aircraft, electrical, and automotive industries, amongst others [1]. In spite of this great success, some of the underlying fundamentals of the spraying processes are still poorly understood [2, 3]: in particular the behavior of the arc inside the torch nozzle for which the anodic root position is determined by the complex balance between gas drag and Lorentz forces [4]. The arc column lengthening leads to an increase of the arc voltage and consecutive restrikes [5] or reconnections of the current channel take place across the surrounding cold gas boundary layer. These periodic phenomena result in strong temperature [6] and velocity [7] oscillations of the outcoming plasma jet. During plasma spraying this may lead to a non-uniform heating and transport of the injected powder particles and consequently adversely affect the quality and yield of the spray deposits [8]. Most of the plasma torches used for thermal spraying, like the Sulzer Metco F4 gun investigated here, require a movement of the anodic arc root over the inner surface of the gun nozzle to distribute the large heat load and consequently increase the anode lifetime. The principle is to force the arc root to move in a controlled way by using, for example, a swirl gas injector [2, 9] or an external magnetic field [10]. Many R&D efforts have been dedicated to new torch designs to reduce [11] or control [12] arc fluctuations and in process control [13] to adjust spray parameters to minimize fluctuations. Systematic studies of the influence of working parameters [14 - 17] on the arc voltage signals and power spectra have shown different operation regimes regarding fluctuations. In addition, the dominant arc fluctuation frequencies can, in some cases, be linked to the electrode wear [14, 15, 18, 19]. Duan et al. have investigated the thickness of the cold gas boundary layer surrounding the arc column by fast, end-on imaging of the torch nozzle exit using a mirror [16, 17]. Their results have shown a dependence of the cold layer thickness on working parameters and a systematic correlation with arc fluctuation regimes.

Despite the above mentioned experimental studies, the basic understanding of the arc behavior still requires further investigations in correlation with advanced modeling and numerical simulations to allow further developments towards improved control, reliability and reproducibility of the existing spraying techniques and for the development of new processes.

In this paper, we present short exposure time, end-on images of the anode interior acquired with an arrangement similar to the one described in reference [16]. The exposure period for image acquisition has been synchronized with several typical features of the arc voltage signal. This allows visualizing the anodic arc attachment behavior throughout the restrike process as presented in section 3.1 below.

In section 3.2, analysis of the images in correlation with the fluctuating signals and of their power spectra is made for various gas flows, currents and for two different types of gas injectors. The effect of electrode wear on the position of the anodic arc root is also presented.

2. EXPERIMENTAL ARRANGEMENT

The atmospheric pressure plasma torch investigated is a Sulzer Metco F4 without powder injection equipped with a 6 mm diam. atmospheric anode nozzle and a thoriated tungsten cathode fitted with either a straight or a swirl (50/50 parallel/tangential flow) gas injector. Typical parameters are: 200 - 800 A current, 20-60 SLPM (Standard Liter per Minute) of Ar as the primary gas with 4 SLPM of H_2 as the secondary gas. The mean electrical power is up to 35 kW with torch efficiency between 30 and 60%. The gun (Figure 1) is mounted on a 2-axis displacement table with the jet axis horizontal.

The arc voltage is measured directly at the gun electrodes with a differential passive voltage probe (÷20, DC-2 MHz). The signal is acquired by a digital oscilloscope LeCroy™ and transferred to a PowerMacintosh™ via a GPIB interface for further analysis using Labview™.

A gated intensified CCD camera (Photonic Science ISIS3) equipped with a 108 mm focal length (FL) lens and a neutral density filter is positioned beside the gun for the imaging of the nozzle exit via a concave mirror (ø 100 mm, FL 50 mm), positioned in front of the gun (Fig. 1). A specially designed mask (cylinder of 6 mm diam., 40 mm length) intercepts the light emitted from the arc column on the torch axis. As illustrated in Figure 2, this device cuts off the brightest emission coming from the hottest plasma region in front of the cathode and allows the camera sensitivity to be increased without saturation, in order to visualize the comparatively weak emission from the anodic arc root at the periphery.

A high voltage pulse/delay generator is used to control both the exposure time (0.5 - 5 µs) of the camera intensifier and the delay with respect to an external "smart" trigger provided by the above mentioned digital oscilloscope (Fig. 1). This arrangement allows the recording of an image taken at a well defined time with respect to a typical feature of the torch voltage signal, such as, for example, a strong voltage drop subsequent to an upstream restrike of the arc [4, 14]. Moreover, the corresponding voltage trace can be acquired simultaneously. The video signal from the CCD camera is recorded with a frame grabber and sequences of synchronized images are stored on a PC.

3. RESULTS AND DISCUSSION

3.1 Anodic arc root imaging throughout the restrike cycle

Previous studies [4, 7, 8, 14 - 17] have shown that the fluctuating behavior of a plasma torch can be characterized by different regimes depending on the gas mixture and current: the restrike regime which prevails for Ar/H_2 mixtures is evidenced by a typical sawtooth shape of the arc voltage signal as shown in Figure 3. The large voltage drops (labeled "1" in Fig. 3) repeat periodically with a frequency between 3 and 4 kHz and have been attributed to "upstream restrikes" [4, 14], for which a breakdown of the arc occurs with a new arc root closer to the cathode. The length of the new arc is strongly reduced, which results in a large drop of the

voltage (30 – 40 V at around 10 MV/s). Between these periodic features there are irregular drops of smaller, amplitude (labeled "2" in Fig. 3). In a previous publication [14], these have been attributed to "downstream restrikes" for which a breakdown of the arc occurs with a new anodic root farther from the cathode or on the diametrically opposite side of the anode. In this case, the new arc termination does not exhibit an S-shape bending which results in a shorter overall length, and leads to a voltage reduction (typically 5 to 15 V at less than 1 MV/s). These small non-periodic voltage drops might also be attributed to short-circuiting of the curved part of the arc at the anode foot [14]. For this phenomenon, which resembles reconnection, the attachment of the anodic root would be maintained at the same position and the arc not interrupted. This interpretation, based only on the time-evolution of the torch voltage and, in some cases, of the corresponding jet light emission [14], suffers from a lack of spatial information. We will show below that time-resolved, end-on imaging of the torch nozzle can help in the interpretation of the restrike phenomena.

In Figure 4 we present images of the anodic arc root attachment at different times within a restrike cycle using the end-on imaging technique of the nozzle exit described in section 2. Eachsub-figure (A, B, C) corresponds to different acquisition times within a typical restrike cycle and show characteristic features: A: before a major restrike, B: after a major restrike, and C: after a minor restrike. Detail of the voltage signals with the exposure time (gate) of the camera (vertical lines) are represented along with the corresponding images of the anodic arc root. Since the camera does not allow for the acquisition of consecutive images within one restrike cycle, the voltage traces are slightly different from one line to the other. However the images and voltage traces shown here are representative of the general features found in a typical restrike cycle such as the one described in Fig. 3.

In Fig. 4 we have also represented circular intensity profiles taken along the contour indicated with the middle white circle on the image of line C. In the following, this polar representation will help to identify the arc root number and locations. This also allows the direct comparison of several images by superimposing their corresponding circular intensity profiles. Moreover a general trend in the anodic arc root behavior can be evidenced by averaging a quite large number of these profiles representing a large number of images, which otherwise would be difficult to present in the frame of a publication.

In Fig. 4 A the image has been acquired just before the large voltage drop corresponding to an "upstream restrike". At this time, the voltage is at its maximum and so is the power dissipated in the arc. There is no clearly defined anodic arc root, which might be because the gas boundary layer temperature is high enough to allow for a diffuse attachment to the anode. We should emphasize that any image acquired several microseconds before major restrikes shows a similar pattern. Since the depth of focus in our imaging conditions exceeds the cathode tip-to-nozzle exit distance, the absence of clear attachment cannot be accounted for by bad focus position.

In Fig. 4 B, which corresponds to about 10 μs after a major restrike, a single new anodic arc root is clearly visible. This is because the temperature of the cold gas boundary layer has now dropped which leads to a constricted and well-delimited current channel to the anode. We

systematically observe a unique arc attachment after major restrikes having a large time derivative of the voltage (around 10 MV/s). This is consistent with the interpretation of upstream restrikes with a new anodic arc attachment closer to the cathode. Moreover, images acquired down to 1 μs after the voltage drop edge already show a single sharp attachment which suggests that, in the case of upstream restrikes, the arc current is transferred within less than 1 μs from the previous diffuse attachment(s) to the new sharp attachment. This is characteristic of a breakdown phenomenon.

In Figure 4 C we present an image taken between two small voltage drops similar to those labeled "2" in Figure 3. There are two distinct arc attachments, which coexist at least during the 1 μs exposure time of the camera. In these conditions, the gas boundary layer temperature is higher than for Fig. 4 B, as evidenced by the halo with cylindrical symmetry around the mask, and by the fact that the voltage is quite high. However, it seems that the conditions required for an upstream restrike to take place are not fulfilled, even if the peak voltages are of the same order of magnitude for the cases A and C (around 80 V). However, the rate of voltage drop in the present case (less than 1 MV/s) is less than in the case of upstream restrikes described above. Note that there is no oscillation on the corresponding voltage signal during the exposure time and within the sampling rate (0.2 μs per point) and voltage probe bandwidth (-3 dB at 2 MHz) used here. A transition from one attachment to the other occurring faster than the bandwidth of the voltage measurement is improbable because we systematically observe multiple attachments between minor restrikes, irrespective of the delay after the first voltage drop. Therefore, our interpretation is that there is creation of a new attachment without immediate destruction of the previous one. It seems that there is a continuous process of creation/vanishing of successive anodic attachment for which we have observed up to three coexisting attachments. It is not yet clear which are the mechanisms that lead to an upstream restrike with a single new arc root instead of multiple co-existing successive attachments. From the spraying point of view, it might be more favorable if the plasma torch could be operated only in the latter mode which resembles a "take-over" mode [4, 14, 16]. However, in most spraying-relevant operation conditions there is a mixture of both phenomena as shown on the voltage signal in Figure 3.

3.2 Effect of external parameters on the anodic arc attachment

It is clear that for the plasma spraying processes, the operation conditions are chosen to obtain the best coating quality and reproducibility. This includes the choice of a plasma gun able to generate the jet parameters most suitable for the type of powders to be sprayed. Moreover, a given plasma torch is designed to operate with specific parameters, such as gas flow and current, which are usually limited to a restricted range for proper operation. In this study, we have deliberately explored the extreme boundaries of the operation parameter space to evidence strong effects and trends. Since the nature of the attachment(s) is strongly dependent on time within a restrike cycle, a systematic study of external parameters is difficult to perform if the

gun is operated in the restrike mode. Therefore this investigation was performed in the take-over mode (without hydrogen) for which the attachment nature depends much less on the time within a voltage oscillation period. Since the anode condition is critical for the behavior of the arc attachment and may, in some cases, dominate the effects of other external parameters such as gas flow or current, we will first present the effect of anode wear.

3.2.1 Effect of anode wear

Figure 5 shows, for two anode conditions, typical end-on images of the anodic attachment along with polar plots showing a superposition of 10 circular intensity profiles and the average over 50 of these profiles. The new anode has operated for about 3 hours with 5 ignitions whereas the so-called "worn anode" has worked for more than 30 hours and shows clear erosion spots. Individual images do not show any significant difference in the attachment nature with anode wear. However, the circular intensity profiles in Fig. 5 give a clear idea of the distribution of the arc root over the inner anode surface. It appears that for a new anode the attachment position is almost distributed over the entire periphery of the anode nozzle, whereas for the worn anode, there is a preferential position in the quadrant 180° to 270°. By inspection of the nozzle interior, this zone revealed pronounced erosion of the anode surface. This means that the anodic attachment tends to occur in regions where the surface is the most eroded and this has strong implications for the anode lifetime. We should note that the torch operation conditions of Fig. 5 are with a low gas flow, moderate current and with the straight gas injector. In the following, it will be shown that the use of a swirl gas injector significantly helps to randomize the location of the attachment over the whole anode surface, if the gas flow is sufficient.

3.2.2 Effect of gas injector geometry

Figure 6 shows typical end-on images that demonstrate the effect of the gas injector geometry on the arc attachment to the anode. For these operation conditions of moderate current and low gas flow, we always observe a single attachment for both injectors. The direction of the arc root is purely radial for the straight injector, whereas it is twisted by the tangential component of the flow for the swirl injector. For some operation conditions, in particular with the use of hydrogen as the secondary gas, the anode foot is constricted and there might be an anode jet. The images of Fig. 6 demonstrate that in the case of a straight gas injector, the anode jet is directed in the radial direction towards the nozzle axis. This effect has been discussed by Duan et al. in reference [17], where they show that it can disturb the arc column by pushing it off axis, therefore favoring a restrike on the opposite side. In the case of a swirl gas injector, the anode jet is directed in the direction of the swirl and therefore its effect on the arc column is less important.

Figure 7 shows another effect of the gas injector geometry on typical end-on images and polar

plots of the circular intensity profiles averaged over 50 images. In contrast with Fig. 6 above, the operation conditions here are with high current and high gas flow (600 A, 60 SLPM Ar). For the swirl injector the anodic arc attachment is no longer clearly defined, and might be of diffuse type, whereas for the straight injector there are clear multiple attachments, which co-exist for the 1 μs exposure time of the camera.

The averages of circular intensity profiles show an almost uniform distribution for the swirl injector, whereas for the straight injector it resembles a flower with eight petals which evidences preferential positions for the attachments. Since the straight injector has eight holes every 45° (position indicated with arrows on Fig. 7) it seems that the arc root tends to be pushed away from the dominant cold gas flow lines exiting the holes.

3.2.3 Effect of gas flow and current

Figure 8 shows images of the anodic arc root(s) in the "current vs. gas flow" operation parameter space. The images of this Figure are representative of the general trends in the anodic attachment behavior for pure argon operation as a function of current and gas flow, when a straight gas injector is used. For low current and low gas flow (Fig. 8C), we always observe a single, well delimited attachment. This is probably because the gas boundary layer is thick and cold due to the low power dissipated in the arc and because the gas flow is not sufficient to create turbulence which would disturb the attachment. If the gas flow is increased (Fig. 8D) some more attachments are created, and up to four can co-exist in our conditions. However these are not permanent in number and position as evidenced by various sequences of images taken randomly which show various numbers of attachments (2 to 4) at different positions. In other words, it seems that there is a continuous process of creation/vanishing of successive attachments at various positions. This behavior might be due to the enhanced turbulence inside the nozzle at high gas flow.

At low gas flow and high current (Fig. 8A), one can observe a single diffuse attachment which is stationary. This corresponds to the so-called "steady mode" [5, 17], for which the voltage signal is very stable (less than 1 % relative fluctuations). For the F4 gun, this mode of operation is usually observed at high current and moderate to low gas flow of pure argon, if the gas injector is straight. It is also favored by a worn anode. If the gas flow is increased at high current (Fig. 8B), the steady mode is lost and the attachment behavior is characterized by well delimited multiple arc roots that co-exist and fluctuate, in a similar manner as for Fig. 8D. However, due to the high current the gas boundary layer is thin and hot, which is evidenced by the bright halo around the mask shadow on Fig. 8B.

If a swirl injector is used, the effect of increasing current on the nature of the arc attachment at high gas flow is different, as illustrated in Figure 9: At low current there are clearly defined multiple co-existing attachments, the same as for the straight injector (Fig. 8D) except that they are twisted by the swirl. However, at high current the attachment seems to be diffuse with no clearly defined current channels through the gas boundary layer which looks thin and hot

because of increased power dissipated in the arc. A consequence is that the fluctuations of the torch voltage are reduced as shown on the power spectra of Figure 10 and in reference [14].

4. CONCLUSIONS

The fluctuating behavior of a DC plasma torch has been investigated using time resolved measurements of the arc voltage coupled with end-on imaging of the electrode gap interior using a gated camera. The anodic arc root attachment has been visualized by using a special mask on the optical path to the camera, which cuts off the dominant emission from the arc column. Series of images have been acquired which are synchronized with typical features in the voltage fluctuation signals, by means of a smart triggering of the camera exposure. An image analysis technique, which extracts circular intensity profiles around the arc column, allows a clear visualization of the arc root(s) attachment position to the anode. Moreover, these circular intensity profiles can be represented and averaged for a large number of images to get a statistical view of the attachment polar distribution.

For the operation of the torch in the restrike mode, the attachment nature strongly depends on the time within the restrike cycle. Three types of attachments have been observed: before major restrikes, the arc root is diffuse which is caused by a thin and hot gas boundary layer which favors the current pathway towards the anode, whereas just after the major restrikes a single, sharp attachment is evidenced throughout a thick and cold gas boundary layer. Between major restrikes which are periodic, there are series of irregular voltage drops of small amplitude during which there is a process of creation/vanishing of multiple attachments with up to three attachments co-existing during the 1 μs exposure time of the camera.

Visualization of the anodic arc root(s) has been investigated as a function of various operation parameters such as electrode wear, gas flow, gas injector type and current. This study has been performed for the case of pure argon flow, for which the attachment nature does not depend on the time within a fluctuation cycle of the take over mode. For worn anodes, the attachment sits preferentially in regions where there is erosion on the anode wall. This has strong consequences on the electrode lifetime, since regions that exhibit wear will be preferentially eroded. However this effect can be attenuated by increasing the gas flow and/or by the use of a swirl gas injector, which help to randomize the attachment position over the inner anode surface. In addition, increasing the gas flow tends to increase the number of attachments, whereas increasing the current leads to a thinner and hotter gas boundary layer, which favors diffuse attachment. At low gas flow and high current the so-called "steady mode " is observed, which is characterized by a single and stable diffuse attachment.

The results presented here reveal the complexity of the nature of the anodic attachment and show, in particular, that any 3D modeling of the arc behavior inside a DC plasma torch should take into account successive creation and vanishing of multiple attachments that may coexist during a significant amount of time.

Acknowledgement

The authors are grateful to Prof. J. Heberlein for stimulating discussions and for his interest in their work. This work was funded by Swiss Federal Research grant CTI No. 4403.1KTS.

References

[1] P. Fauchais and M. Vardelle, *"Plasma Spraying: Present and Future"*, Pure and Appl. Chem. **66** (6), 1247, (1994)

[2] J. -F. Brilhac, B. Pateyron, G. Delluc, J. -F. Coudert, and P. Fauchais, *"Study of the Dynamical and Static Behaviour of DC Vortex Plasma Torches"*, Plasma Chemistry and Plasma Processing **15** (2), 231, (1995)

[3] E. Pfender and C. H. Chang, *"Plasma Spray Jets and Plasma-Particulate Interaction: Modelling and Experiments"*, Proceedings of the 15th International Spray Conference, Nice, France, p. 315, (1998)

[4] J.F. Coudert, M.P. Planche, and P. Fauchais, *"Anode-arc Attachment Instabilities in a Spray Plasma Torch"*, High Temp. Chem. Processes **3**, 639, (1994)

[5] S. A. Wutzke, E. Pfender, and E. R. G. Eckert, *"Study of Electric-arc Behaviour with Superimposed Flow"* , AIAA Journal **5** (4), 707, (1967)

[6] J.F. Coudert and P. Fauchais, "*The Influence of the Arc Fluctuations on the Temperature Measurement in DC Plasma Jets*", High Temp. Chem. Processes **3** (1), 443, (1992)

[7] M.P. Planche, J.F. Coudert, and P. Fauchais, *"Velocity Measurements for Arc Jets Produced by a DC Plasma Spray Torch"*, Plasma Chemistry and Plasma Processing **18** (2), 263, (1998)

[8] P. Fauchais, J.F. Coudert, and M. Vardelle, *"Transient Phenomena in Plasma Torches and in Plasma Sprayed Coating Generation"*, J. Phys. IV France **7**, p. C4-187, (1997)

[9] J. Heberlein, M.P. Planche, Z. Duan, O. Lagnoux, P. Fauchais, and E. Pfender "*Study of Arc Fluctuations with Different Plasma Spray Torch Configurations*", Proceedings of the 13th International Symposium on Plasma Chemistry, edited by C.K. Wu (Beijing, China 1997), vol. III, p. 1460-1465.

[10] V. F. Put'ko, "*Electric Arc Behaviour in Dynamic Magnetic Fields*", in Thermal Plasma and New Materials Technology, vol. 1, Ed. O.P. Solonenko and M. F. Zhukov, Cambridge Interscience Publishing, (1994).

[11] J. Zierhut, P. Haslbeck, K. D. Landes, G. Barbezat, M. Muller, and M. Schutz, "*Triplex –an Innovative Three-Cathode Plasma Torch*", Proceedings of the 15th International Spray Conference, Nice, France, 1998, p.1375.

[12] S. Russ, E. Pfender, and J. Heberlein, *"Anode Arc Attachment Control using Boundary Layer Bleed Holes*, Proceedings of the 1993 National Thermal Spray Conference, Anaheim, CA, USA, p. 97, (1993)

[13] L. Beall, Z. Duan, J. Schein, M. Stachowicz, M. P. Planche, and J. Heberlein, *"Controls for Plasma Spraying based on Plasma Jet Stability Analysis"*, Proceedings of the 15th International Spray Conference, Nice, France, 1998, p. 815

[14] J. -L. Dorier, C. Hollenstein, A. Salito, M. Loch, and G. Barbezat, "*Influence of External Parameters on Arc Fluctuations in a DC Plasma Torch used for Thermal Spraying*", in "Thermal Spray: Surface Engineering via Applied Research", Ed. C. C. Berndt, Pub. ASM International, Material Park, OH, USA, 37, (2000)

[15] J. -L. Dorier, C. Hollenstein, A. Salito, M. Loch, and G. Barbezat, "*Characterisation of Fluctuations in a DC Plasma Torch used For Thermal Spraying*", Proc. of 14th International Symposium on Plasma Chemistry, August 2-6 1999, Prague, Czech Republic, p.331

[16] Z. Duan, K. Wittmann, J.F. Coudert, J. Heberlein, and P. Fauchais, "*Effects of the Cold Gas Boundary Layer on Arc Fluctuations*" Proc. of 14th International Symposium on Plasma Chemistry, August 2-6 1999, Prague, Czech Republic, p.233

[17] Z. Duan and J. Heberlein, "*Anode Boundary Layer Effects in Plasma Spray Torches*", in "Thermal Spray: Surface Engineering via Applied Research", Ed. C. C. Berndt, Pub. ASM International, Material Park, OH, USA, 1, (2000)

[18] J. Xi, G. Krishnappa, and C. Moreau, *"Monitoring of Nozzle Wear during Plasma Spray"*, Proc. of Thermal Spray: A United Forum for Scientific and Technological Advances, C.C. Berndt (Ed.), ASM International, USA, 1997, p.413

[19] Z. Duan, L. Beall, M. P. Planche, J. Heberlein, E. Pfender, and M. Stachowicz, *"Arc Voltage Fluctuations as an Indication of Spray Torch Anode Condition"*, Proc. of Thermal Spray: A United Forum for Scientific and Technological Advances, C.C. Berndt (Ed.), ASM International, USA, 1997, p.407

FIGURE CAPTION

Figure 1: Top view of the experimental arrangement with the image synchronization circuit.

Figure 2: End-on images of the torch showing the anode nozzle with the cathode tip inside (A), the arc column without mask (B) and the anodic attachment with the mask (C). The outer grey circle delimits the nozzle hole whereas the inner one demarcates the effective shadow of the mask (exposure time 1 μs).

Figure 3: Typical voltage trace in the restrike mode, showing periodic large voltage drops (labeled "1"), with smaller, irregular voltage drops in between (labeled "2").

Figure 4: Voltage signals with exposure time and corresponding end-on images of the nozzle exit for three different characteristic features of the restrike cycle: just before (A) and 10 μs after (B) a major restrike, and after minor restrikes (C). The polar plots represent circular intensity profiles (taken along the middle white line indicated on the last image). Plasma conditions: 500 A, 4/40 SLPM H_2/Ar, straight injector, worn electrodes, exposure time 1 μs.

Figure 5: Effect of anode wear illustrated by end-on images of the anodic arc attachment, superposition of 10 circular intensity profiles and the average over 50 of such profiles. Operation conditions: 300 A, 30 SLPM Ar, straight injector, 2 μs exposure time.

Figure 6: End-on images of the anodic arc attachment for the swirl and straight gas injectors. Operation conditions: 300 A, 30 SLPM Ar, new electrodes, 3 μs exposure time.

Figure 7: Typical images and polar plots of the circular intensity profiles of the anodic arc attachment for the swirl and straight gas injectors. Each plot corresponds to the average over 50 different intensity profiles. The arrows indicate the position of the eight gas injection holes of the straight injector. Operation conditions: 600 A, 60 SLPM Ar, new electrodes, 1 μs exposure time.

Figure 8: Typical end-on images of the torch nozzle illustrating the general trends in the nature of anodic attachment(s) as a function of gas flow and current. Operation parameters : 200 A (A and C), 600 A (B and D), 20 SLPM Ar (C and D), 60 SLPM Ar (A and B), straight injector, worn electrodes, exposure time : 1 μs (A and B), 2 μs (C and D).

Figure 9: Typical images and polar plots of the circular intensity profiles of the anodic arc attachment for low current (A: 200 A) and high current (B: 600 A). Each polar plot corresponds to the average over 50 different intensity profiles. Operation conditions: 60 SLPM Ar, new electrodes, swirl injector, exposure time: 2 μs (A), 1μs (B).

Figure 10: Power spectra of the voltage fluctuations in the operation conditions of Fig. 9.

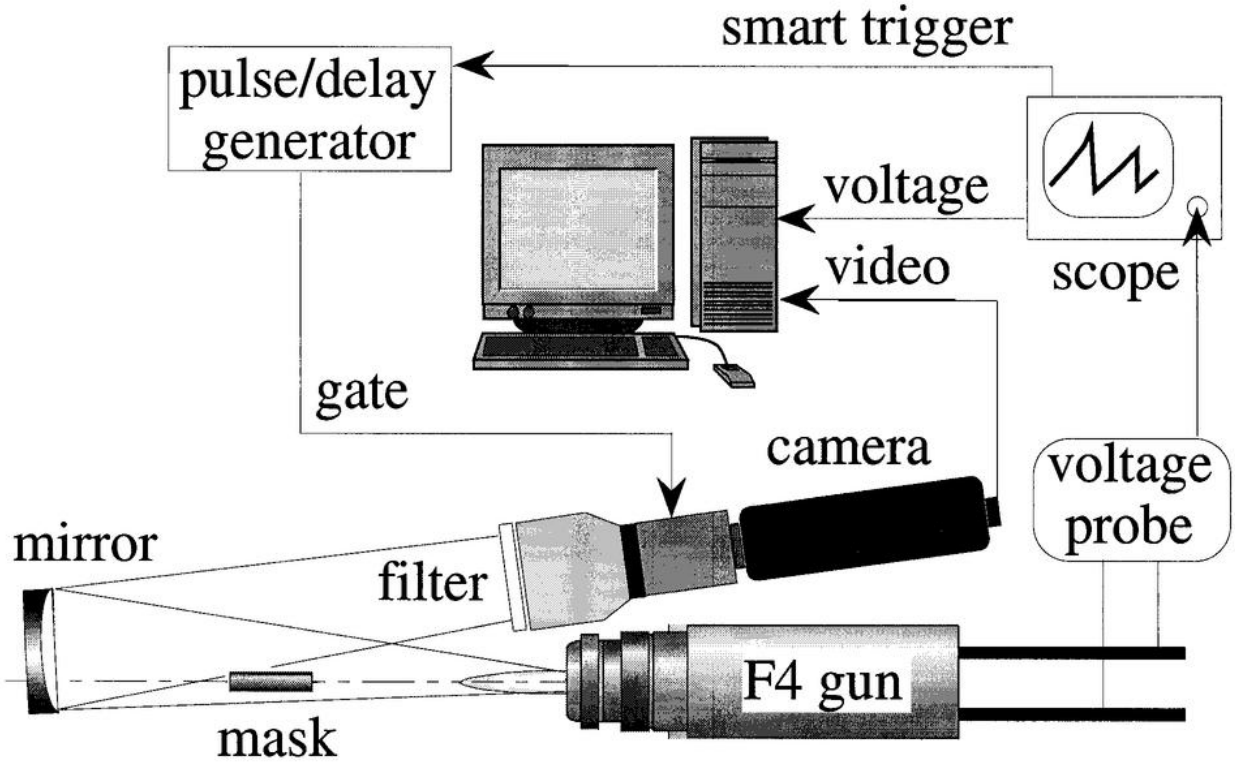

J.-L Dorier et al.
"Time-resolved Imaging of Anodic..."

Fig. 1 of 10

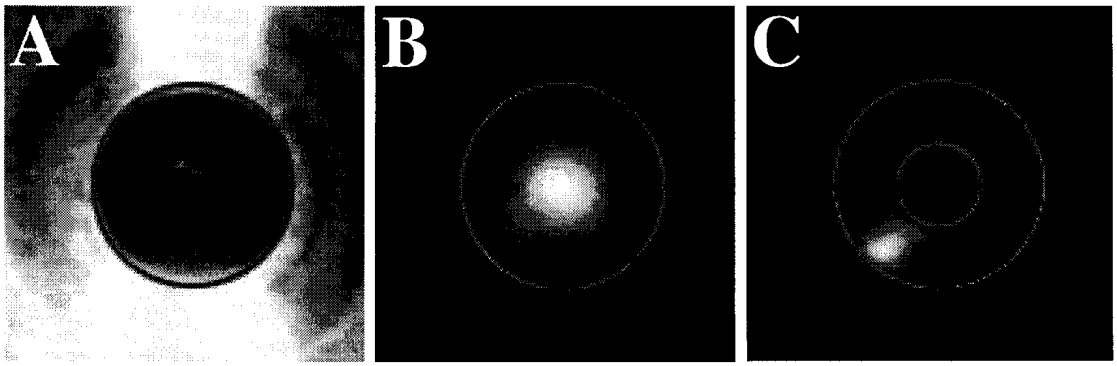

J.-L Dorier et al.
"Time-resolved Imaging of Anodic..."

Fig. 2 of 10

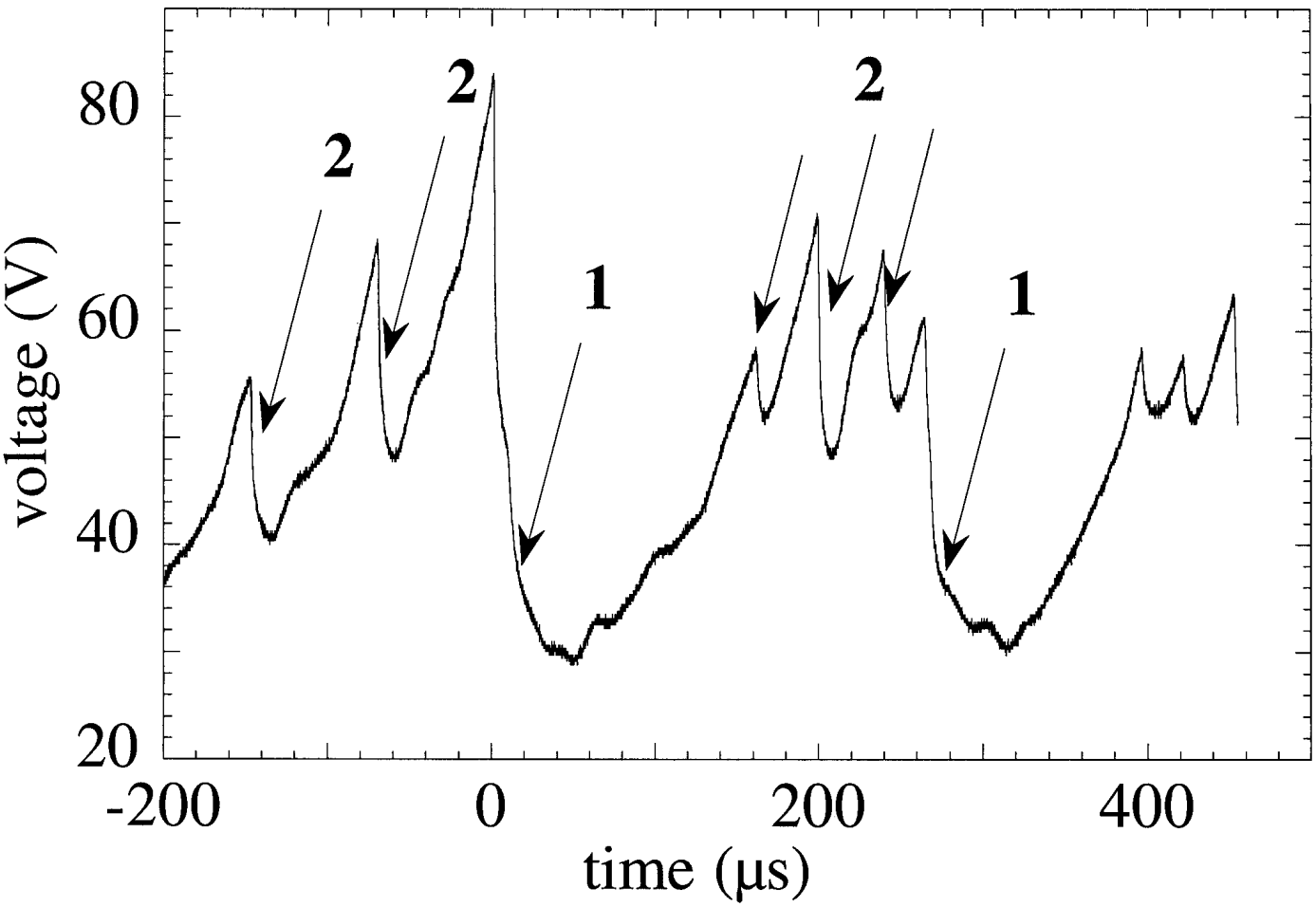

J.-L Dorier et al.
"Time-resolved Imaging of Anodic..."

Fig. 3 of 10

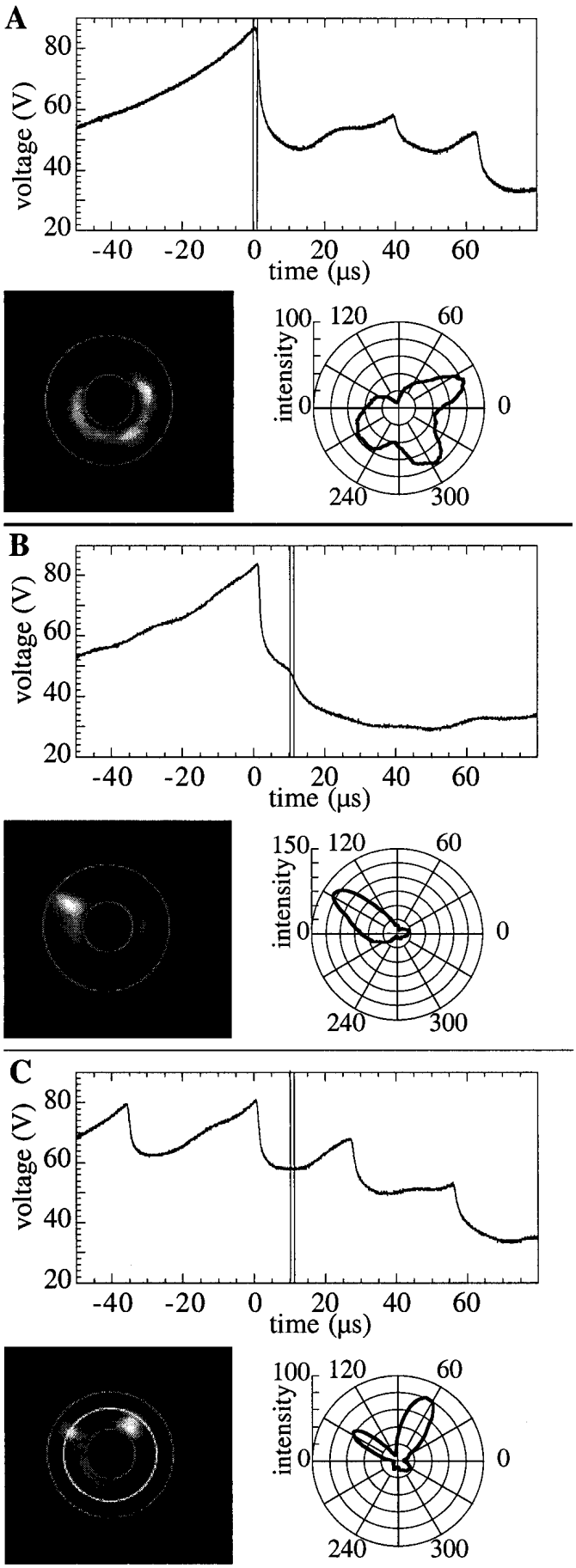

J.-L. Dorier et al.

" Time-resolved Imaging of Anodic..:"

Fig. 4 of 10

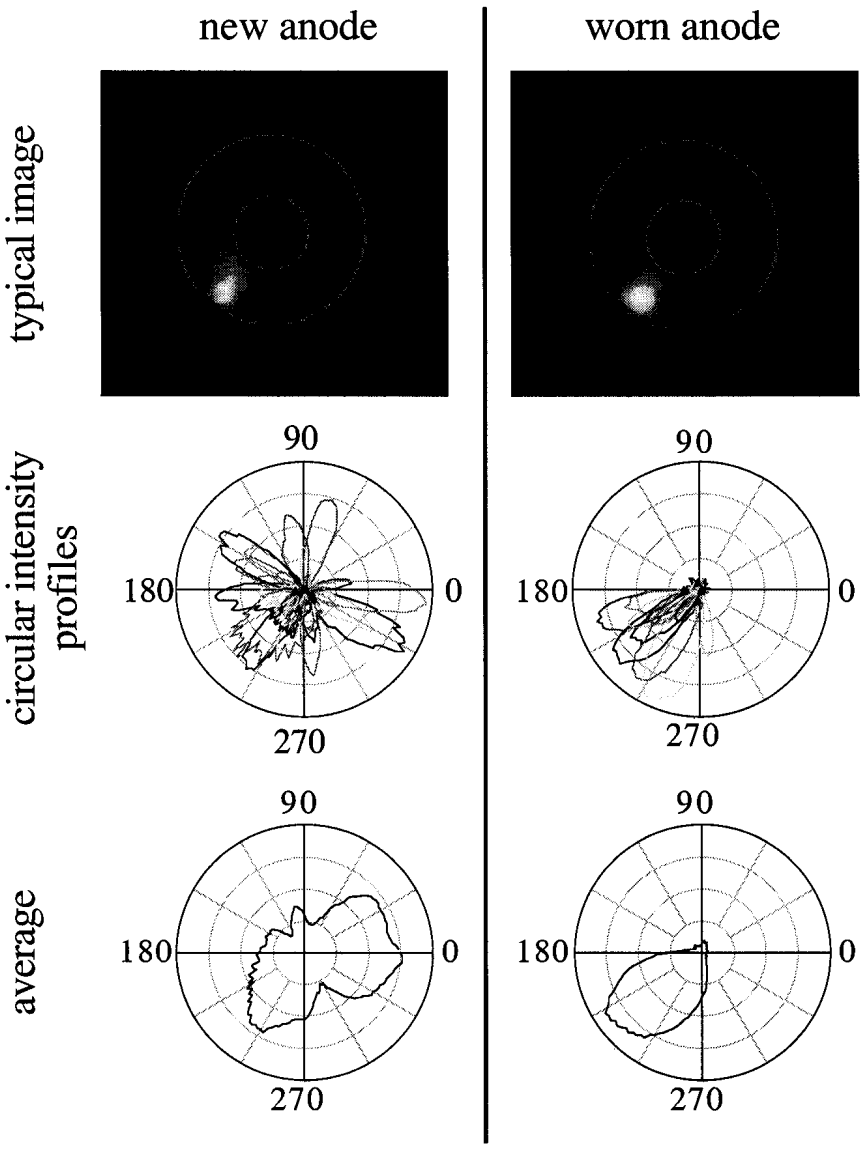

J.-L. Dorier et al.

" Time-resolved Imaging of Anodic..:"

Fig. 5 of 10

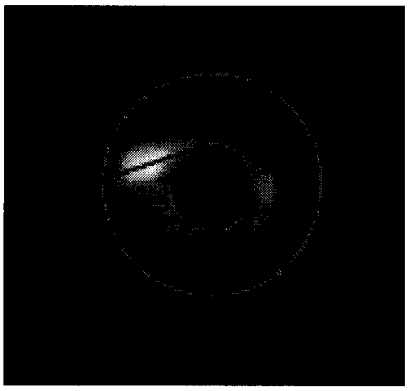

swirl

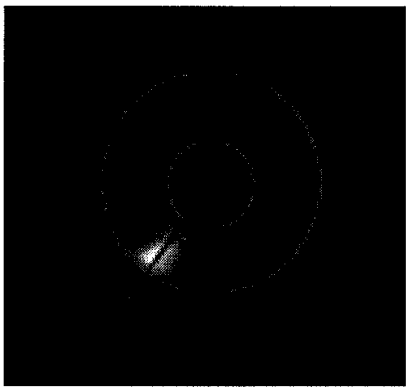

straight

J.-L. Dorier et al.

" Time-resolved Imaging of Anodic..:"

Fig. 6 of 10

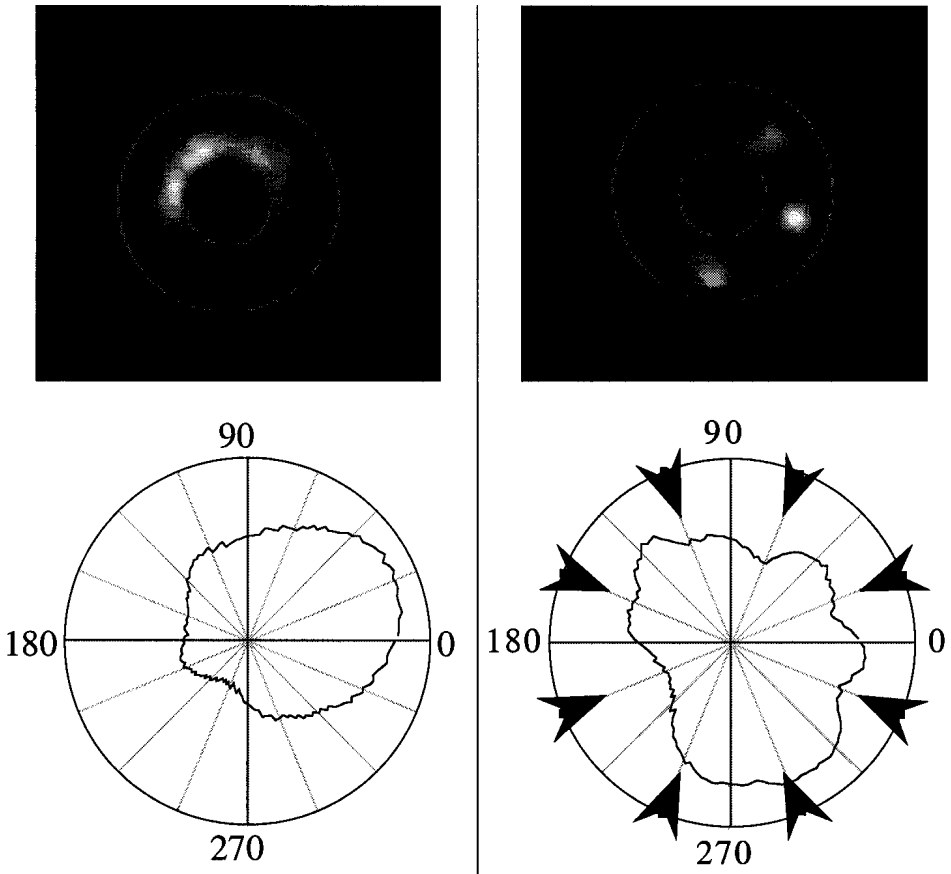

J.-L. Dorier et al.

" Time-resolved Imaging of Anodic..:"

Fig. 7 of 10

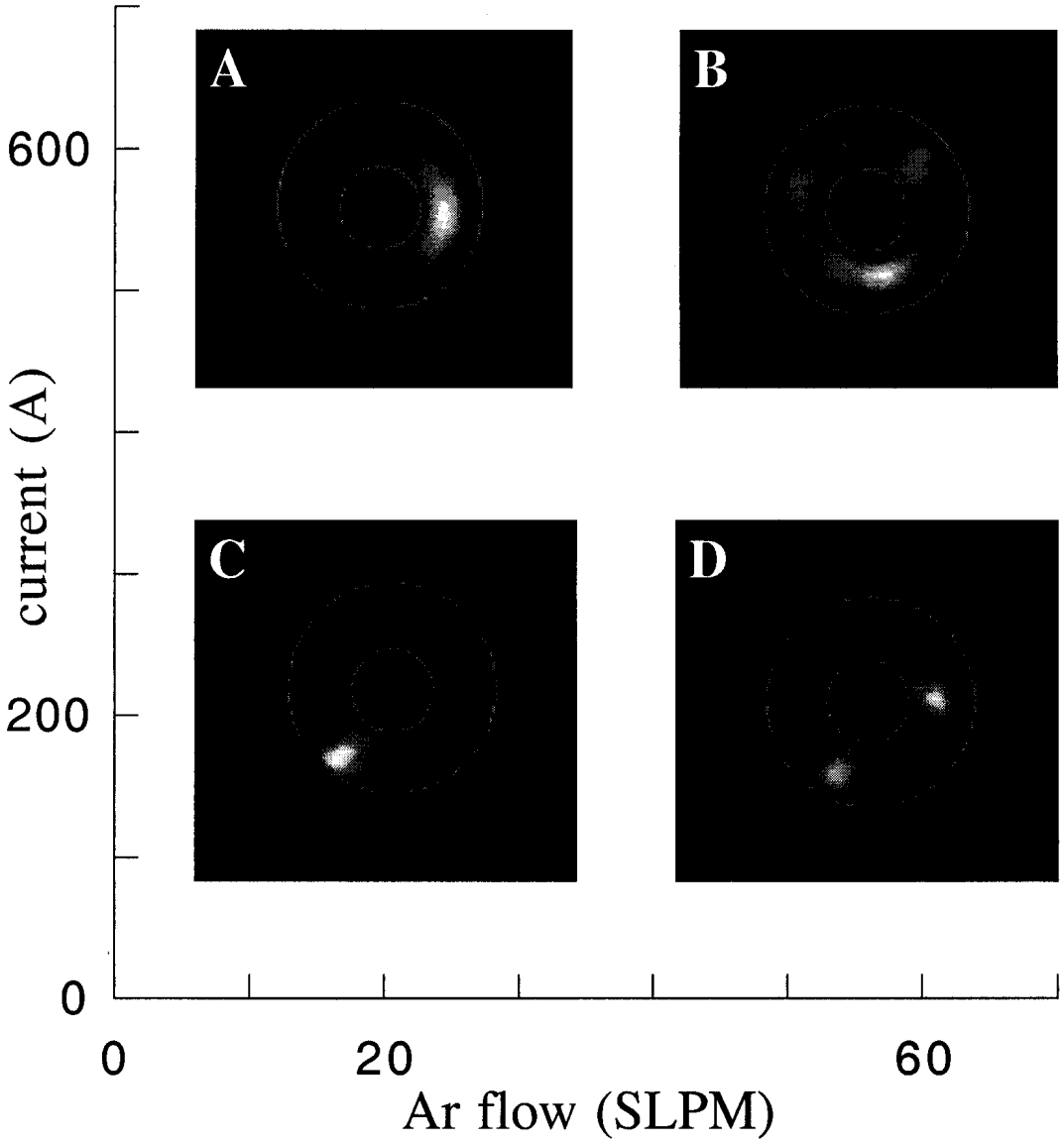

J.-L Dorier et al.
"Time-resolved Imaging of Anodic..."

Fig. 8 of 10

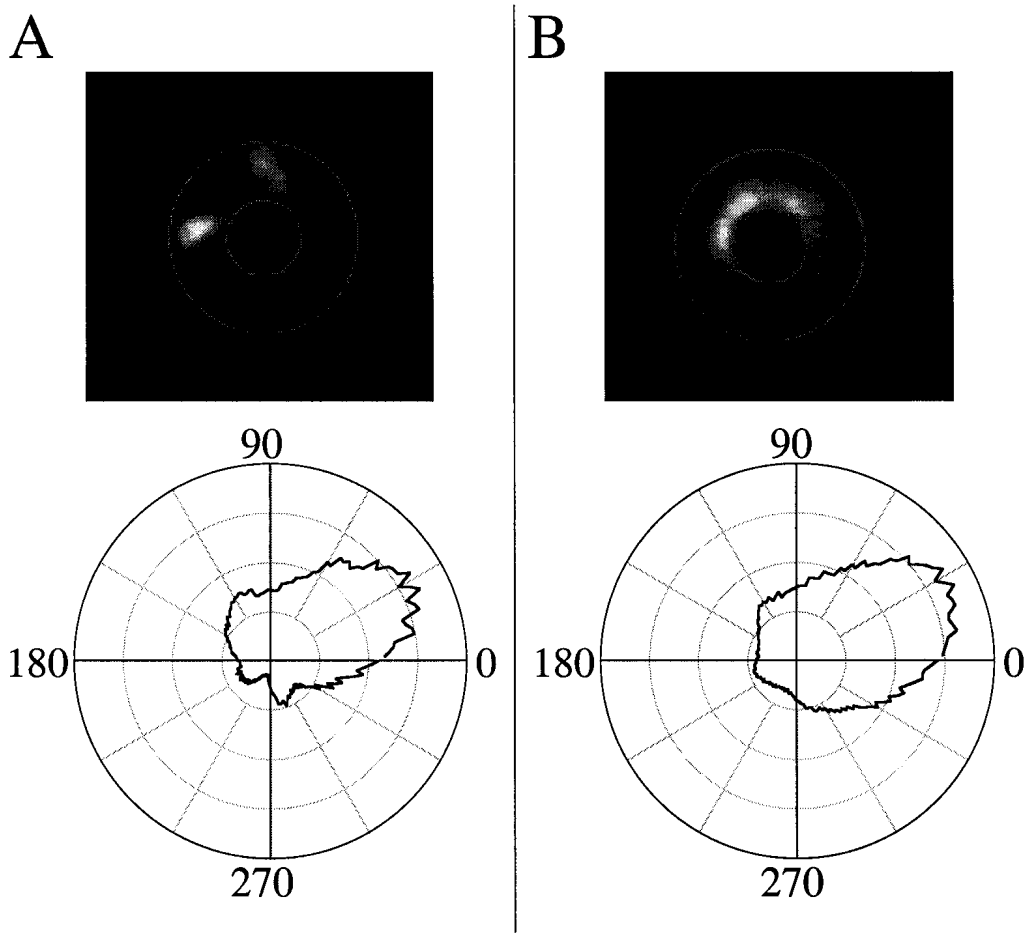

J.-L. Dorier et al.

" Time-resolved Imaging of Anodic..:"

Fig. 9 of 10

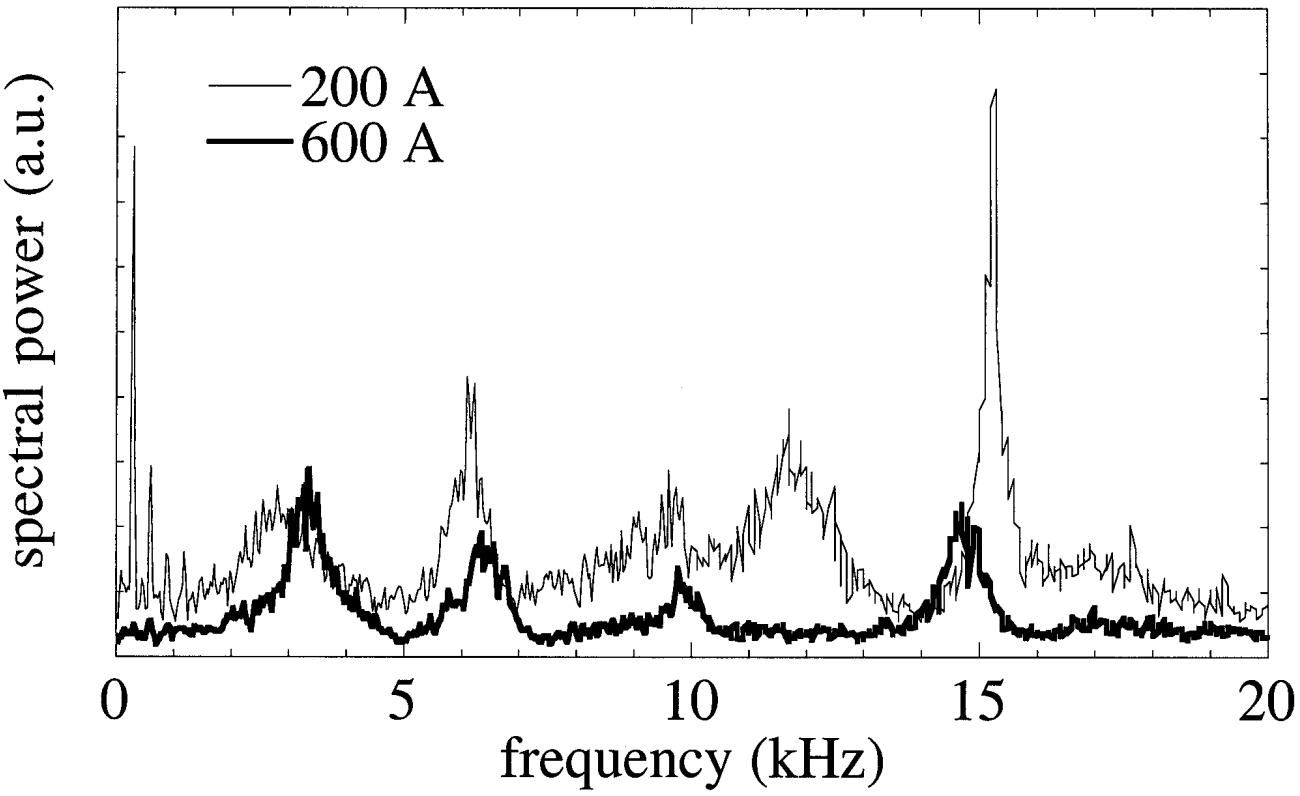

J.-L Dorier et al.
"Time-resolved Imaging of Anodic..."

Fig. 10 of 10